Inorg. Chem. **2006**, *45*, 8655–8663

Catalysts for Monooxygenations Made from Polyoxometalate: An Iron(V)–Oxo Derivative of the Lindqvist Anion

Etienne Derat,[†] Devesh Kumar,[†] Ronny Neumann,[‡] and Sason Shaik*,[†]

Department of Organic Chemistry and the Lise Meitner-Minerva Center for Computational Quantum Chemistry, Hebrew University of Jerusalem, Givat Ram Campus, 91904 Jerusalem, Israel and Department of Organic Chemistry, The Weizmann Institute of Science, Rehovot, 76100 Israel

Received June 11, 2006

This work uses density functional calculations to design a new high-valent Fe(V)═O catalyst $[Mo_5O_{18}Fe{=}O]^{3-}$, which is based on the Lindqvist polyoxometalate ($Mo_6O_{19}^{2-}$). Because the parent species is stable to oxidative conditions, one may assume that the newly proposed iron–oxo species will be stable, too. The calculated Mössbauer spectroscopic data may be helpful toward an eventual identification of the species. The calculations of C–H hydroxylation and C═C epoxidation of propene show that, if made, $[Mo_5O_{18}Fe{=}O]^{3-}$ should be a potent oxidant that will be subject to strong solvent effect. Moreover, the Lindqvist catalyst leads to an intriguing result; the reaction that starts along an epoxidation pathway with C═C activation ends with a C–H hydroxylation product (**^{4}6**) due to rearrangement on the catalyst. The origins of this result are analyzed in terms of the structure of the catalyst and the electronic requirements for conversion of an epoxidation intermediate to a hydroxylation product. Thus, if made, the $[Mo_5O_{18}Fe{=}O]^3$ will be a selective C–H hydroxylation reagent.

Introduction

Polyoxometalates (POMs) constitute a diverse class of inorganic oxo−metal clusters with defined structures based on octahedra of tungstic and/or molybdic oxides such as the $PW_{12}O_{40}^{3-}$ Keggin-type species in Scheme 1A, which possesses a central phosphate moiety that coordinates the edge-sharing WO_6 octahedra into a single cluster, or the Lindqvist type depicted in Scheme 1B, which possess only six transition metals placed in the corners of an octahedron and linked to a central oxygen atom shared among the six metal ions.[1] The stability of these compounds under strongly oxidizing conditions has made POMs extremely attractive as oxidation catalysts and for activation of environmentally benign oxidants.[2] The art of functionalizing of POMs is well developed, and many motifs of the general structure in Scheme 1A have been made.[3] One of the modes of functionalization is the replacement of the native metal ions, W (Mo), by transition metals (TM) to create POM−TM (M = Fe, Ru, Mn, etc) species, which exhibit improved catalytic behaviors in a variety of oxidative processes. For example, Keggin-type POM−Fe(III) and especially Keggin-

Scheme 1. Structures of Polyoxometalate Complexes. (A) A Keggin-Type with a Central Phosphate. (B) A Lindqvist Type with a Central Oxygen Atom

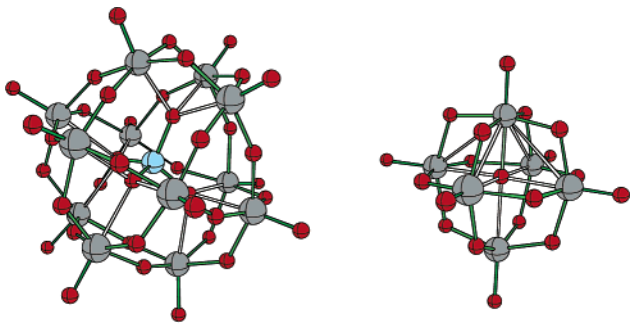

* To whom correspondence should be addressed. E-mail: sason@yfaat.ch.huji.ac.il. Tel +972 (0)2 658 5909. Fax +972 (0)2 658 4033.
[†] Hebrew University of Jerusalem.
[‡] The Weizmann Institute of Science.

(1) (a) Pope, M. T. In *Isopoly and Heteropoly Anions*; Springer: Berlin, Germany, 1983. (b) *Polyoxometalate Chemistry*; Pope, M. T.; Müller, A., Eds.; Kluwer Academic: Dordrecht, The Netherlands, 2001.
(2) (a) Kozhevnikov, I. V. In *Catalysis by Polyoxometalates*; Wiley: Chichester, England, 2002. (b) Hill, C. L.; Prosser-McCartha, C. M. *Coord. Chem. Rev.* **1995**, *143*, 407. (c) Mizuno, N.; Misono, M. *Chem. Rev.* **1998**, *98*, 199. (d) Neumann, R. *Prog. Inorg. Chem.* **1998**, *47*, 317.
(3) Rhule, J. T.; Hill, C. L.; Judd, D. A.; Schinazi, R. F. *Chem. Rev.* **1998**, *98*, 327−358.

10.1021/ic0610435 CCC: $33.50
Published on Web 09/16/2006

type POM−Mn(III), which in the presence of oxygen surrogates such as PhIO, perform monooxygenation of organic molecules[2,3] in a manner analogous to the high-valent iron−oxo species in heme enzymes and in metalloporphyrin complexes[4] or in the nonheme Que reagents.[5] Indeed, as recently demonstrated by means of density functional theoretic (DFT) calculations, both Keggin-type POM−$Fe^{V}O$ and Keggin-type POM−$Mn^{V}O$ should be capable of hydroxylating C−H bonds and epoxidizing C=C bonds with relative ease.[6] This was confirmed experimentally, and it was shown that while the Keggin-type POM−$Mn^{V}O$ is highly reactive, the Keggin-type POM−$Fe^{V}O$ is nonreactive because it forms a persistent complex with the PhI. Thus, the POM−TM appears to be a promising platform for discovering new catalysts.[7] One of the goals of the present paper is to propose a new C−H activation catalyst based on the Lindqvist type POM with the hope of inducing the interplay of theory and experiment in this discovery-oriented research field.[3,7]

The Lindqvist anions, $M_6O_{19}^{2-}$ (M = Mo, W), Scheme 1B, are among the smallest members of the POM family.[8] These anions, which exhibit high point group symmetry (O_h), are highly stable in condensed phase and even in the gas phase.[9] DFT is one of many methods of addressing this stability,[10] and it is thought to originate in the aromaticity of the M_4O_4 rings of the Lindqvist anion.[11] There is considerable knowledge about how to functionalize these anions and form arylimido derivatives[12] including the recently

Scheme 2. Hydroxylation and Epoxidation of Propene by $[Mo_5O_{18}Fe{=}O]^{3-}$ Studied by Means of DFT Calculations

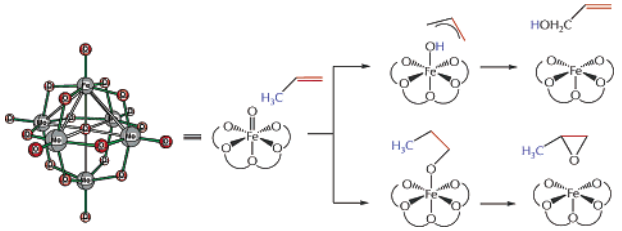

made fluorinated organoimido hexamolybdates.[13] Thus, we considered an iron derivative of the Lindqvist anion, $[Mo_5O_{18}Fe{=}O]^{3-}$, as a potential candidate for a new family of oxidation catalysts and studied its properties and reactivity using DFT calculations. To compare the reactivity of $[Mo_5O_{18}Fe{=}O]^{3-}$ to the previously studied[6,14] $[PW_{11}O_{39}Fe{=}O]^{3-}$, we used propene as a substrate that can undergo both C=C epoxidation and allylic C−H hydroxylation, as indicated in Scheme 2.

Methods

Following previous studies,[6,14] the $[Mo_5O_{18}Fe{=}O]^{3-}$ species was generated from $[Mo_6O_{19}]^{2-}$ by replacing a single $[Mo^{VI}{=}O]^{2+}$ group with $[Fe^{V}{=}O]^{3+}$. The oxidation state of the iron(V) corresponded to the same effective oxidation state of Compound I species[4] in which $Fe^{IV}{=}O$ was coordinated to a porphyrin radical cation. Whereas the truncation of $[Mo^{VI}{=}O]^{2+}$ left behind a lacunary $[Mo_5O_{17}]$,[6−] the combination of this lacunary with the $[Fe^{V}{=}O]^{3+}$ fragment generated the $[Mo_5O_{18}Fe{=}O]^{3-}$ species with a total charge of −3. This structure is referred to as $POM_5{-}FeO^{3-}$, while the previously calculated Keggin-type reagent is referred to as $POM_{11}{-}FeO^{4-}$; the POM subscripts indicate the respective number of Mo or W atoms in the cluster.

All the structures were calculated by DFT using the unrestricted hybrid functional UB3LYP[15] and the double-ζ effective core potential basis set LACVP,[16] henceforth B1. Some tests were run also with the OPBE functional, which recently was demonstrated to accurately reproduce spin states of Fe(II) complexes.[17] The results of both functionals were virtually the same.

On the basis of the greater speed of JAGUAR[18] compared with GAUSSIAN[19] in geometry optimization procedures, we used JAGUAR for that purpose and subsequently employed GAUSSIAN 98 or 03 for analytic frequency calculations. DFT calculations of POM derivatives are gradually appearing more frequently in the

(4) (a) *Cytochrome P450: Structure, Mechanism, and Biochemistry*, 2nd ed.; Ortiz de Montellano, P. R., Ed.; Plenum Press: New York, 1995. (b) *Cytochrome P450: Structure, Mechanism, and Biochemistry*, 3rd Ed.; Ortiz de Montellano, P. R., Ed.; Kluwer Academic/Plenum Publishers: New York, 2004. (c) Poulos, T. L. In *The Porphyrin Handbook*; Kadish, K. M.; Smith, K. M., Guilard, R., Eds.; Academic Press: New York, 2000; Vol. 4, p 190. (d) Groves, J. T. *Proc. Natl. Acad. Sci. U.S.A.* **2003**, *100*, 3569. (e) Sono, M.; Roach, M. P.; Coulter, E. D.; Dawson, J. H. *Chem. Rev.* **1996**, *96*, 2841. (f) For a recent Ruthenium−oxo catalyst with a high turnover number for C−H hydroxylation, see: Wang, C.; Shalyaev, K. V.; Bonchio, M.; Carofiglio, T.; Groves, J. T.; *Inorg. Chem.* **2006**, *45*, 4769−4782 and references therein.

(5) Kaizer, J.; Klinker, E. J.; Oh, N. Y.; Rohde, J.-U.; Song, W. J.; Stubna, A.; Kim, J.; Munck, E.; Nam, W.; Que, L., Jr. *J. Am. Chem. Soc.* **2004,** *126*, 472−473.

(6) Kumar, D.; Derat, E.; Khenkin, A. M.; Neumann, R.; Shaik, S. *J. Am. Chem. Soc.* **2005**, *127*, 17712−17718.

(7) Anderson, T. M.; Neiwert, W. A.; Kirk, M. L.; Piccoli, P. M. B.; Schultz, A. J.; Koetzle, T. F.; Musaev, D. G.; Morokuma, K.; Cao, R.; Hill, C. L. *Science* **2004**, *306*, 2074−2077.

(8) (a) Lindqvist, I. *Ark. Kemi* **1950**, *5*, 247. (b) Allcock, H. R.; Bissell, E. C.; Shawl, E. T. *Inorg. Chem.* **1973**, *12*, 2963. (c) Fuchs, J.; Feiwald, W.; Hartl, H. *Acta Crystallogr., Sect. B* **1978**, *34*, 1764.

(9) (a) Yang, X.; Waters, T.; Wang, X.-B.; O'Hair, R. A. J.; Wedd, A. G.; Li, J.; Dixon, D. A.; Wang, L.-S. *J. Phys. Chem. A.* **2004,** *108*, 10089−10093. (b) Lau, T.-C.; Wang, J.; Guevremont, R.; Siu, K. W. M. *Chem. Commun.* **1995**, 877. (c) Deery, M. J.; Howarth, O. W.; Jennings, K. R. *J. Chem. Soc., Dalton Trans.* **1997**, 4783. (d) Walanda, D. K.; Burns, R. C.; Lawrance, G. A.; von Nagy-Felsobuki, E. I. *J. Chem. Soc., Dalton Trans.* **1999**, 311.

(10) (a) Li, J. *J. Cluster Sci.* **2002**, *13*, 137. (b) Bridgeman, A. J.; Cavigliasso, G. *Inorg. Chem.* **2002**, *41*, 1761. (c) Bridgeman, A. J.; Cavigliasso, G. *J. Phys. Chem. A* **2003**, *107*, 4568.

(11) (a) King, R. B. *Inorg. Chem.* **1991**, *30*, 4437. (b) Cai, T.; Chen, Z. D.; Wang, X. Z.; Li, L. M.; Lu, J. X. *Prog. Nat. Sci.* **1997**, *7*, 554. (c) see ref 9a.

(12) (a) Wei, Y.; Xu, B.; Barnes, C. L.; Peng, Z. *J. Am. Chem. Soc.* **2001**, *123*, 4083−4084. (b) Wei, Y.; Meng, L.; Cheung, C. F.-C.; Barnes, C. L.; Peng, Z. *Inorg. Chem.* **2001**, *40*, 5489−5490. (c) Wu, P. F.; Li, Q.; Ge. N.; Wei, Y.; Wang, Y.; Wang, P.; Guo, H. *Eur. J. Inorg. Chem.* **2004**, 2819−2822.

(13) Xue, S.; Ke, S.; Yan, L.; Cai, Z.; Wei, Y *J. Inorg. Biochem.* **2005**, *99*, 2276−2281.

(14) de Visser, S. P.; Kumar, D.; Neumann, R.; Shaik, S. *Angew. Chem., Int. Ed.* **2004**, *43*, 5661.

(15) (a) Becke, A. D. *J. Chem. Phys.* **1992**, *96*, 2155. (b) Becke, A. D. *J. Chem. Phys.* **1992**, *97*, 9173. (c) Becke, A. D. *J. Chem. Phys.* **1993**, *98*, 5648. (d) Lee, C.; Yang, W.; Parr, R. G. *Phys. Rev. B* **1988**, *37*, 785.

(16) (a) Hay, J. P.; Wadt, W. R. *J. Chem. Phys.* **1985**, *82*, 299−308. (b) Friesner, R. A.; Murphy, R. B.; Beachy, M. D.; Ringlanda, M. N.; Pollard, W. T.; Dunietz, B. D.; Cao, Y. X. *J. Phys. Chem. A* **1999**, *103*, 1913−1928.

(17) (a) Handy, N. C.; Cohen, A. J. *Mol. Phys.* **2001**, *99*, 403. (b) Perdew, J. P.; Burke, K.; Ernzerhof, M. *Phys. Rev. Lett.* **1996**, *77*, 3865. (c) Fouqueau. A.; Casida, M.; Daku, L. M. L.; Hauser, A.; Neese, F. *J. Chem. Phys.*, **2005**, *122*, 044110−13.

(18) *Jaguar 5.5*; Schrödinger, Inc.: Portland, OR, 2003.

(19) (a) Frisch, M. J.; et al. *Gaussian 98*, Revision A.07, Gaussian, Inc.: Pittsburgh, PA, 1998. (b) Frisch, M. J.; et al. *Gaussian 03*, Revision B.05, Gaussian, Inc.: Pittsburgh, PA, 2003.

current literature,[20] which demonstrates that the method is both pragmatic and reasonably reliable.

Reaction pathways were verified by a scan along a given coordinate while optimizing freely all other coordinates. Single point calculations were carried out on the optimal species with the larger basis set, LACV3P+*(iron)/6-311+G*(rest), henceforth B2, for energy evaluation. These calculations were labeled as B2//B1.

The effect of solvent was estimated with the model implemented in JAGUAR5.5, by using two different solvents; one is acetonitrile, which is commonly used for experimental studies, and the other is a less polar solvent (chlorobenzene), which is commonly used in our theoretical studies of P450 reactions.[6] The solvent was characterized by two properties: a dielectric constant, ϵ, and a probe radius, r. For acetonitrile, $\epsilon = 37.5$, $r = 2.2$ Å, while for chlorobenzene, $\epsilon = 5.7$, $r = 2.7$ Å.

Since Mössbauer spectroscopy is commonly used to characterize iron complexes and to distinguish between different oxidation states of iron, we carried out Mössbauer calculations of the POM_6-FeO^{3-} complex. The calculations were carried out with program ORCA[21] using the recommended basis set and procedures.[22]

The data are summarized in the Supporting Information.

Results

Properties of $[Mo_5O_{18}Fe{=}O]^{3-}$. The $[Mo_5O_{18}Fe{=}O]^{3-}$ reagent, henceforth POM_5-FeO^{3-}, was found to possess an Fe(V) center with a d^3 electronic configuration and two closely lying spin states, a quartet and a doublet. The d-block orbitals are depicted in Figure 1, and are shown to split into the familiar three-below-two pattern typical of an octahedral complex. The lowest three orbitals are derived from the t_{2g} set and involve antibonding interactions between the 3d orbitals on iron and the corresponding 2p orbitals on the oxo ligand (with some contribution from the cage oxygens) and are labeled as π^*_{xz}, π^*_{yz}, and δ. The higher two orbitals are derived from the e_g set and are labeled as $\sigma^*_{z^2}$ and $\sigma^*_{x^2-y^2}$. The lower set of orbitals are singly occupied in the lowest two states as indicated in Figure 1. The ground state is the quartet state that lies below the doublet by ca. 11−13 kcal/mol. These values were checked with UOPBE.[17] In that case, the quartet state was found to lie below the doublet by 13.53/13.47 kcal/mol, respectively, with UOPBE/LACVP//UB3LYP/LACVP and full optimization at the UOPBE/LACVP level.

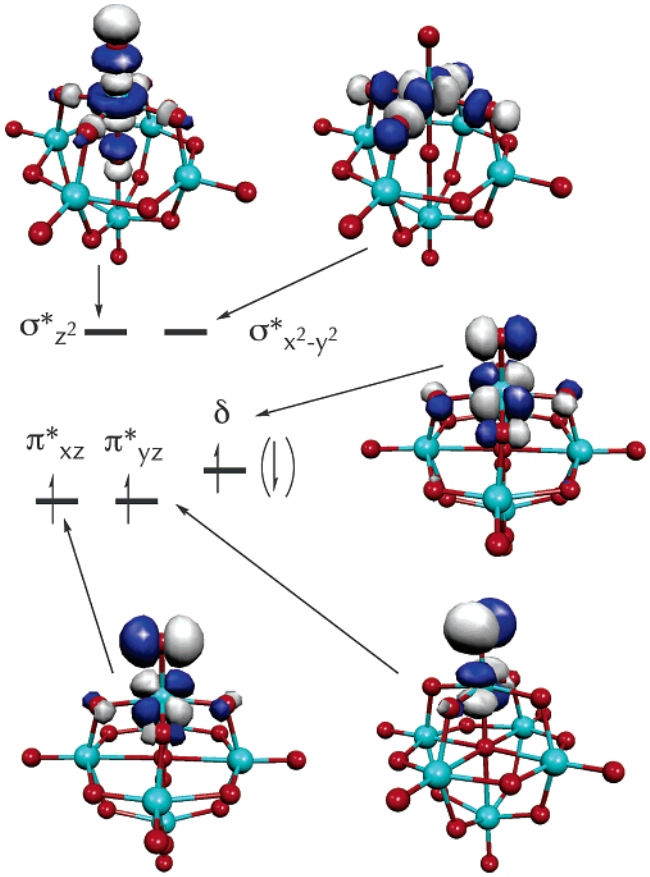

Figure 1. Graphical representation of the three singly occupied orbitals in the Lindqvist type anion $^{4,2}[POM_5FeO]^{3-}$. Two electrons are in π^* type orbitals and the third one in the δ orbital. This last one has some mixing with π^*_{xz} and can be spin up or down.

The significant energy gap projects the role of d−d exchange[23] that stabilizes the quartet state relative to the open-shell doublet state. Other spin states were tried, for example, a doublet state with $\delta^1\pi^{*2}$ configuration, but calculations show that this state is 11.54 kcal/mol higher than the open-shell doublet state described above.

The key geometric features of the two states are shown in Figure 2 along with group spin densities. In both cases, the FeO distance is 1.67 and 1.69 Å, which is typical to high-valent iron−oxo reagents (1.646 Å in ref 24a, 1.65 Å in ref 25c),[24] and, for example, is comparable to the recently postulated nonheme $Fe^{V}O$ species.[25] The Mo−O distances are comparable to the X-ray data available for the pristine Lindqvist anion.[26] The spin density (ρ) distribution shows a

(20) See for example: (a) Bagno, A.; Bonchio, M.; Sartorel, A.; Scorrano, G. *ChemPhysChem.* **2003,** *4*, 517. (b) Maestre, J. M.; Lopez, X.; Bo, C.; Poblet, J.-M.; Casan-Pastor, N. *J. Am. Chem. Soc.* **2001**, *123*, 3749. (c) Tsipis, A.; Tsipis, C. A. *J. Phys. Chem. A,* **2000**, *104*, 859. (d) Rohmer, M.-M.; Bénard, M.; Cadot, E.; Secheresse, F. In *Polyoxometalate Chemistry;* Pope, M. T.; Müller, A., Eds.; Kluwer Academic Publ.: The Netherlands, 2001, p 117. (e) Duclusaud, H.; Boshch, S. A. *Inorg. Chem.* **1999**, *38*, 3489. (f) Duclusaud, H.; Boshch, S. A. *J. Am. Chem. Soc.* **2001**, *123*, 2825. (g) Bridgeman, A. *Chem.—Eur. J.* **2004**, *10*, 2935. (h) Musaev, D. G.; Morokuma, K.; Geletii, Y. V.; Hil, C. L. *Inorg. Chem.* **2004,** *43*, 7702. (i) For a recent interplay of DFT and experiment, see: Anderson, T. M.; Cao, R.; Skolnikna, E.; Hodgson, K..O.; Hardcastle, K. I.; Neiwert, W. A.; Wu, S.; Kirk, M. L.; Knottenbelt, S.; Depperman, E. C.; Keita, B.; Nadjo, L.; Musaev, D. G.; Morokuma, K.; Hill, C. L. *J. Am. Chem. Soc.*, **2005**, *127*, 11948.

(21) Neese, F. *ORCA*, Version 2.4; Revision 10; Max-Planck-Institut für Bioanorganische Chemie: Mülheim a. d. Ruhr, Germany, 2004

(22) The procedures and basis set (on Fe) for calculating Mössbauer parameters with ORCA are taken from Neese, F. *Inorg. Chim. Acta* **2002**, *337*, 181−192. The SV(P) basis set was used (Schäfer, A.; Horn, H.; Ahlrichs, R. *J. Chem. Phys.* **1992**, *97*, 2571−2577), but because the description of the core orbitals is especially important the basis set was fully decontracted.

(23) Carter, E. A.; Goddard, W. A., III. *J. Phys. Chem.* **1988**, *92*, 5679−5683.

(24) (a) Rohde, J.-U.; In, J.-H.; Lim, M. H.; Brennessel, W. W.; Bukowski, M. R.; Stubna, A.; Münck, E.; Nam, W.; Que, L. Jr. *Science* **2003**, *299*, 1037−1039. (b) Groves, J. T. *Proc. Natl. Acad. Sci. U.S.A.* **2003**, *100*, 3569. (c) Stone, K. L.; Behan, R. K.; Green, M. T. *Proc. Natl. Acad. Sci. U.S.A.* **2005**, *102*, 16563−16565.

(25) (a) Ogliaro, F.; de Visser, S. P.; Groves, J. T.; Shaik, S. *Angew. Chem., Int. Ed.* **2001**, *40*, 2874. (b) Bassan, A.; Blomberg, M. R. A.; Siegbahn, P. E. M.; Que, L., Jr. *J. Am. Chem. Soc.* **2002**, *124*, 11056−11063.

(26) (a) Guo, Y.; Wang, X.; Li, Y.; Wang, E.; Xu, L.; Hi, C. *J. Coord. Chem.* **2004**, *57*, 445−451. (b) Shi, Y.; Yang, W.; Xue, G.; Hu, H.; Wang, J. *J. Mol. Struct.* **2006**, *784*, 244−248. (c) Dolbecq, A.; Guirauden, A.; Fourmigué, M.; Boubekeur, K.; Batail, P.; Rohmer, M.-M.; Bénard, M.; Coulon, C.; Sallé, M.; Blanchard, P. *J. Chem. Soc., Dalton Trans.* **1999**, 1241−1248.

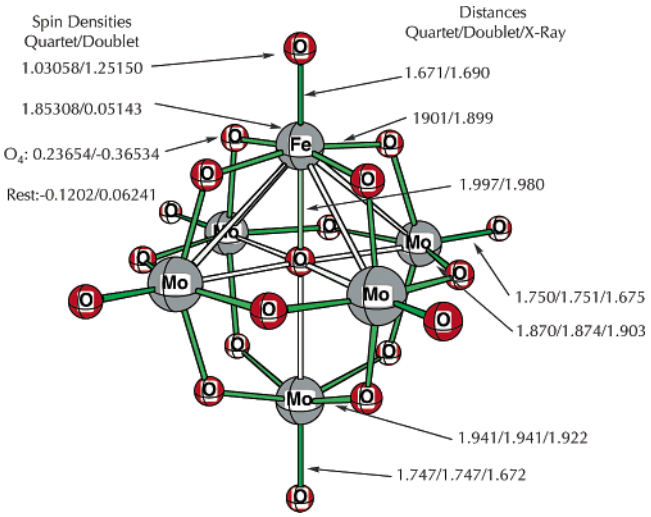

Figure 2. Key geometric details (in Å) and spin density (ρ) distribution in the quartet and doublet state of $[POM_5FeO]^{3-}$. The geometric details of the pristine $[Mo_6O_{19}]^{2-}$ anion (see ref 12c) are indicated as the third entry wherever appropriate.

Table 1. Calculated Mössbauer Parameters and Relative Energies for $[POM_5FeO]^{3-}$ in the Doublet and Quartet States[a]

spin states	η	ΔE_Q (mm/s)	δ (mm/s)	ΔE, kcal/mol
doublet	0.002	−1.995	0.0356	0.0
quartet	0.009	−1.979	−0.0137	−13.9

[a] The relative energy between the two spin states is calculated using the large basis set taken for the Mössbauer calculations.

good deal of spin delocalization from the central iron ion to its close coordination sphere. The spin on the iron in the quartet state is 1.85, and the remaining 1.15 spins are distributed over the oxo moiety of the Fe=O bond and the other five ligands. In the doublet state, the spin on Fe is very small, because in addition to spin delocalization to the coordination sphere the iron spin density is reduced because of the down-electron in the δ orbital, which partially cancels the spin up contribution from the other two electrons in the π^* orbitals.

Table 1 collects the Mössbauer isomer shifts, quadrupole splittings, and asymmetry parameters for $[POM_5FeO]^{3-}$. Because there are no experimental data for this theoretically designed species, we may attempt to compare the values to literature data for heme complexes.[27] Thus, the asymmetry parameter is low, which indicates an octahedral environment of the iron. The quadrupole splitting is larger than known data for Compound I species of heme complexes[27] or of the Que compounds in nonheme iron−oxo reagents.[28] The isomer shift, which is known to be sensitive to the oxidation state, is calculated to be nearly zero and smaller than similar values obtained for Compound I of P450 and HRP.[27,29] This signifies that the oxidation state of iron in $[POM_6FeO]^{3-}$ is

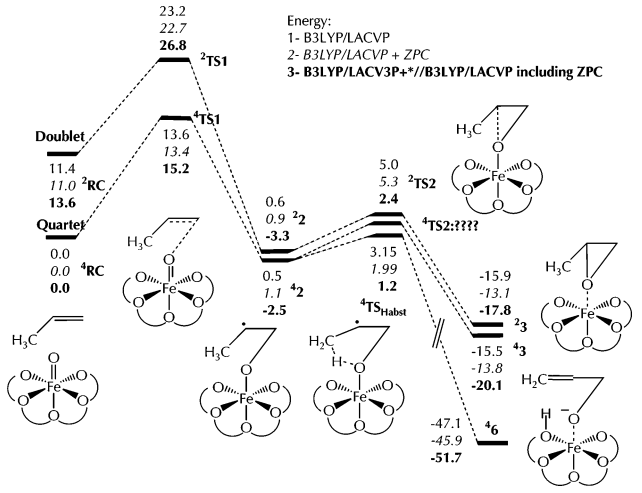

Figure 3. Energy profile for the epoxidation pathway of propene by $[POM_5FeO]^{3-}$ at different levels (see methods section).

greater than in heme Compound I. The values for $[POM_5FeO]^{3-}$ seem unique enough to suggest that the species may be identified by Mössbauer spectroscopy.

Energy Profiles During C=C Epoxidation of Propene. Figure 3 depicts the energy profile for the epoxidation of propene, while Figure 4 shows the optimized structures of the critical species. The energy profile shows a typical epoxidation mechanism observed for iron−oxo reagents[30] with a bond activation phase leading to two radical complex intermediates, ^{4,2}**2**, followed by a ring closure step to furnish the epoxide complexes ^{4,2}**4**. Nevertheless, there are two interesting features, which need further elaboration. Although initially the two states of the complex of POM_6FeO^{3-} with propene (^{4,2}**RC**) are widely separated by 13.6 kcal/mol (at the best level), at the intermediate stage the two states become almost degenerate, and then again at the product stage, the states again are widely separated in energy.

The second noteworthy feature in Figure 3 is associated with the behavior of the ^{4}**2** radical-complex. Instead of ring closure to yield the epoxide complex, the iron−oxo alkyl undergoes internal H-atom transfer from the methyl group to an equatorial oxo ligand and produces the alkoxy complex of an allylic hydroxylation product with a protonated equatorial oxygen ligand, ^{4}**6**. The structures of the critical species in Figure 4 show the changes in bond lengths as expected from the double bond activation and then ring closure. The Lindqvist catalyst leads to an intriguing result; a reaction that starts with C=C activation along an epoxidation pathway and terminates in a C−H hydroxylation product (^{4}**6**).

Energy Profiles During Allylic C−H Hydroxylation of Propene. The energy profile for allylic hydroxylation of propene by POM_6-FeO^{3-} is shown in Figure 5, while the

(27) Schünemann, V.; Winkler, H. *Rep. Prog. Phys.* **2000**, *63*, 263−353.
(28) (a) Rohde, J.-U.; In, J.-H.; Lim, M. H.; Brennessel, W. W.; Bukowski, M. R.; Stubna, A.; Münck, E.; Nam, W.; Que, L., Jr. *Science* **2003**, *299*, 1037−1039. (b) Rohde, J.-U.; Torelli, S.; Shan, X.; Lim, M. H.; Klinker, E. J.; Kaizer, J.; Chen, K.; Nam, W.; Que, L., Jr. *J. Am. Chem. Soc.* **2004**, *126*, 16750−16761. (c) Sastri, C. V.; Park, M. J.; Ohta, T.; Jackson, T. A.; Stuibna, A.; Seo, M. S.; Lee, J.; Kitagawa, T.; Munck, E.; Que, L., Jr.; Nam, W. *J. Am. Chem. Soc.* **2005**, *127*, 12494−12495.
(29) (a) Derat, E.; Cohen, S.; Shaik, S.; Altun, A.; Thiel, W. *J. Am. Chem. Soc.* **2005**, *127*, 13611−13621. (b) Schöneboom, J. C.; Neese, F.; Thiel, W. *J. Am. Chem. Soc.* **2005**, *127*, 5840−5853.
(30) (a) Shaik, S.; Kumar, D.; de Visser, S. P.; Altun, A.; Thiel, W. *Chem. Rev.* **2005**, *105*, 2279−2328. (b) de Visser, S. P.; Ogliaro, F.; Sharma, P. K.; Shaik, S. *J. Am. Chem. Soc.* **2002**, *124*, 11809−11826. (c) Kumar, D.; de Visser, S. P.; Sharma, P. K.; Derat, E.; Shaik, S. *JBIC, J. Biol. Inorg. Chem.* **2005**, *10*, 181−189. (d) Kamachi, T.; Yoshizawa, K. *J. Am. Chem. Soc.* **2003,** *125*, 4652−4661.

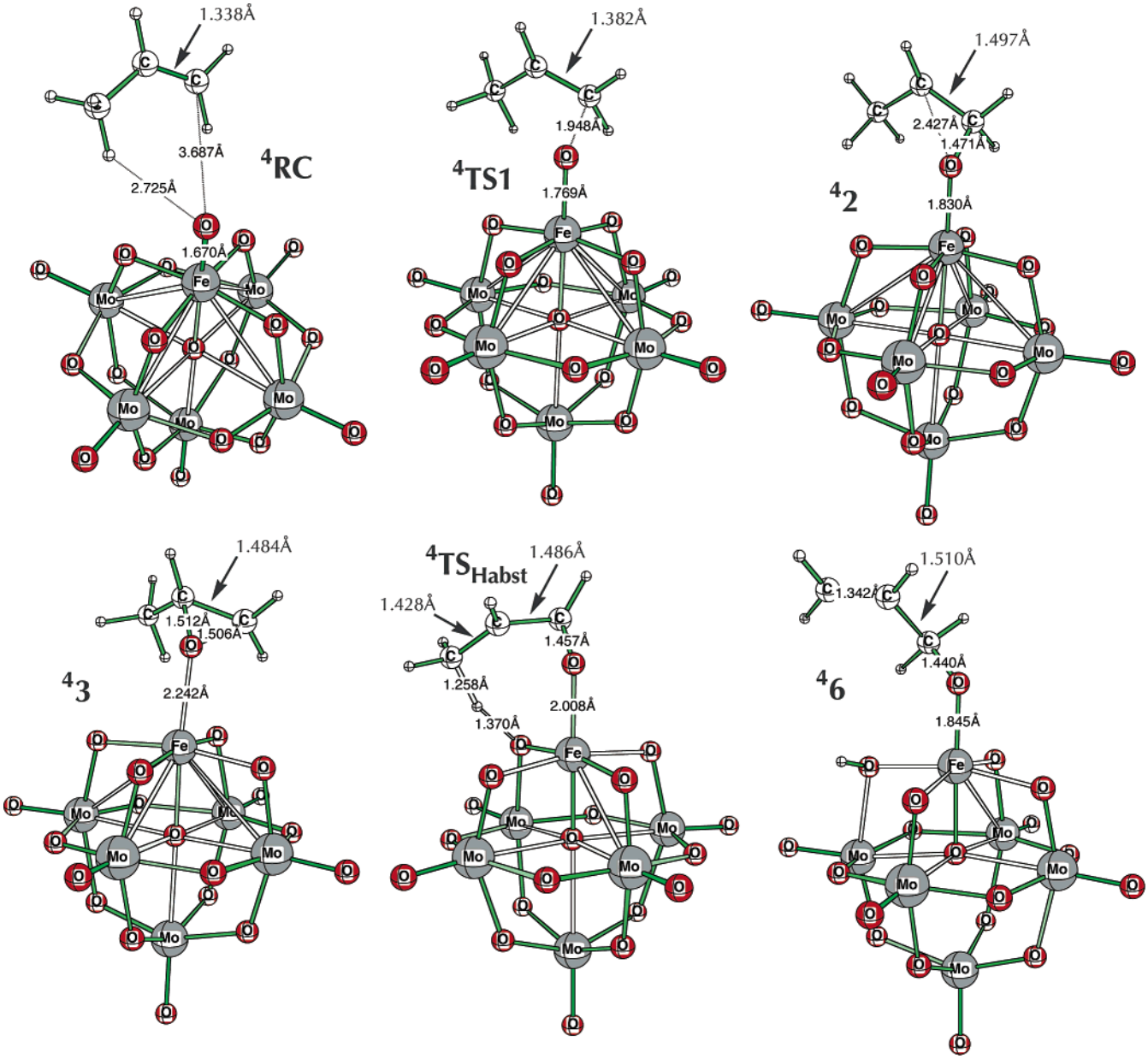

Figure 4. Structures obtained at the B3LYP/LACVP level in the quartet state for the epoxidation process (that result in hydroxylation product). Key distances are given in Å.

optimized geometries of the critical structures are depicted in Figure 6. The hydroxylation profile follows the typical rebound mechanism.[30,31] Initially, the iron−oxo reagent abstracts the allylic hydrogen and forms the radical complexes in the doublet and quartet states. Subsequently, the allyl radical rebounds and forms the ferric−alcohol complexes ^{4,2}**5**. Once again, the quartet and doublet states, which start initially with a large gap, collapse at the stage of the radical intermediates, and the spin state gap increases past the rebound. The geometries of the structures in Figure 6 reflect a rebound mechanism involving H-abstraction followed by radical rebound.[31] Interestingly, the allylic hydroxylation product ^{4}**5** exhibits a geometry that is inclined toward abstraction of the hydroxylic H by one of the equatorial oxo ligands of the POM_6−Fe fragment that leads eventually to the ^{4}**6** complex, which is formed during C═C activation as discussed above.

Integrated Energy Profiles for Propene Oxidation and Solvent Effects. Figure 7 shows the integrated energy profiles (at the common highest level) for the oxidation, and it is apparent that the trends are very similar at the lowest and highest computational levels. The hydroxylation process has a slightly lower barrier than epoxidation mainly because of the zero point energy correction, which is larger for hydroxylation because of the loss of a C−H bond in the transition state.

Table 2 lists the B2//B1 bond activation barriers in the gas phase and in two solvents. The barriers are presented in two values separated by a slash, $\Delta E^{\ddagger}(^{4}\mathbf{R})/\Delta E^{\ddagger}(^{4}\mathbf{RC})$; the first value is relative to the separate reactants, ^{4}**R**, and the second

(31) Groves, J. T.; McClusky, G. A. *J. Am. Chem. Soc.* **1976**, *98*, 859−861.

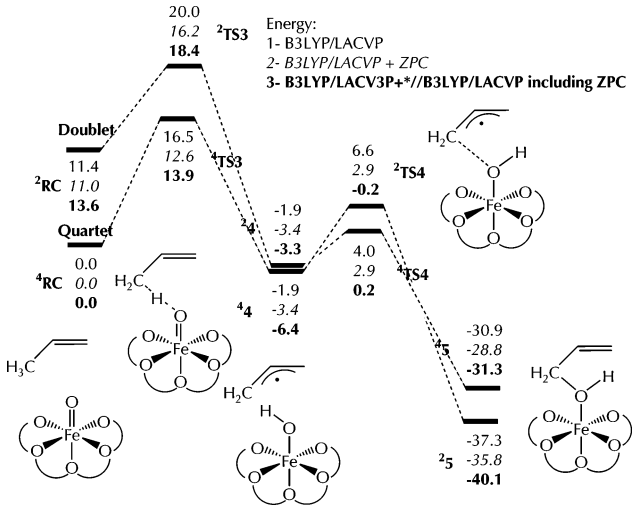

Figure 5. Energy profile for the hydroxylation pathway of propene by $[POM_5FeO]^{3-}$ at different levels (see methods section).

is relative to the **^{4}RC** clusters. The zero point energy correction (ZPC) and solvation corrections were evaluated at the B1 level, and the increments were added to the B2 single point energies (see Supporting Information for total energies). By comparing the barriers from the **^{4}RC** cluster in the gas phase and in acetonitrile, it is seen that the solvent effect is quite large and reaches 8.1−9.3 kcal/mol for the quartet process. On the doublet surface, the solvation lowers the hydroxylation transition states **^{2}TS3** species below the respective cluster, **^{2}RC**, while the epoxidation species, **^{2}TS1** is only 1.3 kcal/mol higher than the cluster (see Supporting Information). Thus, in both the quartet and the doublet surface, the barriers become small, and the $Mo_5O_{18}FeO^{3-}$ becomes a potentially powerful oxidant. This large solvent effect was noted before[6] for the $POM_{11}O_{40}$−FeO^{3-} oxidant and would require some rationale. The conclusion concerns energy barriers only and does not consider entropic effects, which might be very large for these highly charge species.

Interaction of the POM_5FeO^{3-} Reagent with Aryl Iodides. One way of generating iron−oxo species is by use of oxygen surrogates such as PhI═O or generally ArI═O, which transfers an oxygen atom to the iron to generate the oxo−iron species.[33] More recently, it was proposed that the PhI molecule can remain attached to the iron−oxo and affect its reactivity.[34,35] This was found in our previous study of $[PW_{11}O_{39}Fe{=}O]^{3-}$ in which pentaflurophenyl iodide formed a persistent complex with the reagent that gave characteristic NMR signals.[6] To test the situation with the Lindqvist catalyst, we calculated the complexation energies of Ph-I and F_5Ph-I with $Mo_5O_{18}FeO^{3-}$. The results are shown in Table 3. These results show that the complexation energy is large with F_5Ph−I, but it is moderate with Ph−I. We concluded that this trend must be electrostatic since there was no significant charge-transfer either from the ArI to the iron−oxo or vice versa. Indeed, the positive charge on iodine is enhanced in F_5PhI vs PhI (e.g., the B2 charges on iodine in F_5PhI are 0.593/0.596 for doublet/quartet states vs 0.483/0.491 in PhI). In addition, the total charge on the carbon atoms of the phenyl ring is quite different for the two substrates; it is negative for Ph-I and positive for F_5Ph−I (e.g., the total B2 charge on the six carbon atoms in Ph-I doublet/quartet states is −1.65562/-1.67393 compared with 0.19094/0.19359 in F_5Ph−I). These positive charges on F_5-Ph-I interact favorably with the large negative charge of the $Mo_5O_{18}FeO^{3-}$ species.

We further note that the complexation energy of Ph−I with the oxo−iron reagent is slightly weaker than that of propene with the reagent. Ph−I═O or even Tol-I═O may be able to transfer oxygen to the $POM_5O_{18}Fe^{III}(H_2O)^{3-}$ species and create a weak $Mo_5O_{18}FeO^{3-}$/I−Ph complex; in turn, the Ph−I molecule can be displaced by propene that will undergo rapid oxidation.

Discussion

Figure 7 contains a few features, two of which are outstanding: (a) the low barriers in a solvent such as acetonitrile promise that the Lindqvist catalyst will be a powerful oxidant, and (b) the new catalyst is predicted to generate C−H hydroxylation products irrespective of the initial identity of the bond that is being activated (C−H or C═C). A third feature concerns the quartet−doublet energy gap, which decreases from the reactants toward the radical complex intermediates (**^{2,4}2** and **^{2,4}4**) and then increases again. This decrease of the gap means that essentially there will be a tendency for two-state reactivity (TSR)[36,37] albeit dominated by the quartet state reaction.

TSR Features. The changes in the quartet−doublet energy gap reflect the changes in the orbitals of the reactants along the reaction path. Figure 8 depicts an orbital evolution diagram that shows these transformations for the two spin states. The changes in the diagram are based on the oxidation state formalism[30a] and refer to C−H hydroxylation where the substrate is represented by the doubly occupied orbital, σ_{CH}, of the oxidizable C−H bond. Thus, initially the oxo−iron(V) reagent possesses two oxidation equivalents above the product state (Fe^{III} complexes, **3**−**6** in Figure 7), and

(32) Hirao, H.; Kumar, D.; Thiel, W.; Shaik, S. *J. Am. Chem. Soc.* **2005**, *127*, 13007−13018.
(33) Ortiz de Montellano, P. R. In *Cytochrome P450*; 1st ed.; Ortiz de Montellano, P. R., Ed.; Plenum Publishers: New York, 1987; pp 217−271.
(34) Collman, J. P.; Chien, A. S.; Eberspacher, T. A.; Brauman, J. I. *J. Am. Chem. Soc.* **2000**, *122*, 11098−11100.
(35) (a) Nam, W.; Choi, S. K.; Lim, M. H.; Rohde, J. U.; Kim, I.; Kim, J.; Kim, C.; Que, L., Jr. *Angew. Chem., Int. Ed.* **2003**, *42*, 109−111. (b) Suh, Y.; Seo, M. S.; Kim, M.; Kim, Y. S.; Jang, H. G.; Tosha, T.; Kitagawa, T.; Kim, J.; Nam, W. *J. Inorg. Biochem.* **2006**, *100*, 627−633.
(36) (a) Shaik, S.; Danovich, D.; Fiedler, A.; Schröder, D.; Schwarz, H. *Helv. Chem. Acta* **1995**, *78*, 1393−1407. (b) Schröder, D.; Shaik, S.; Schwarz, H. *Acc. Chem. Res.* **2000**, *33*, 139−145. (b) Ogliaro, F.; Harris, N.; Cohen, S.; Filatov, M.; de Visser, S. P.; Shaik, S. *J. Am. Chem. Soc.* **2000**, *122*, 8977−8989. (c) Shaik, S.; Cohen, S.; de Visser, S. P.; Sharma, P. K.; Kumar, D.; Kozuch, S.; Ogliaro, F.; Danovich, D. *Eur. J. Inorg. Chem.* **2004**, *35*, 207−226. (d) de Visser, S. P.; Ogliaro, F.; Sharma, P. K.; Shaik, S. *J. Am. Chem. Soc.* **2002**, *124*, 11809−11826. (e) Kumar, D.; de Visser, S. P.; Sharma, P. K.; Cohen, S.; Shaik, S. *J. Am. Chem. Soc.* **2004**, *126*, 1907−1920.
(37) For some applications and generalizations in organometallic chemistry see: (a) Harvey, J. N.; Aschi, M. *Faraday Discuss.* **2003**, *124*, 129−143. (b) Poli, R.; Harvey, J. N. *Chem. Soc. Rev.* **2003**, *32*, 1−8. (c) Harvey, J. N.; Poli, R.; Smith, K. M. *Coord. Chem. Rev.* **2003**, *238*, 347−361.

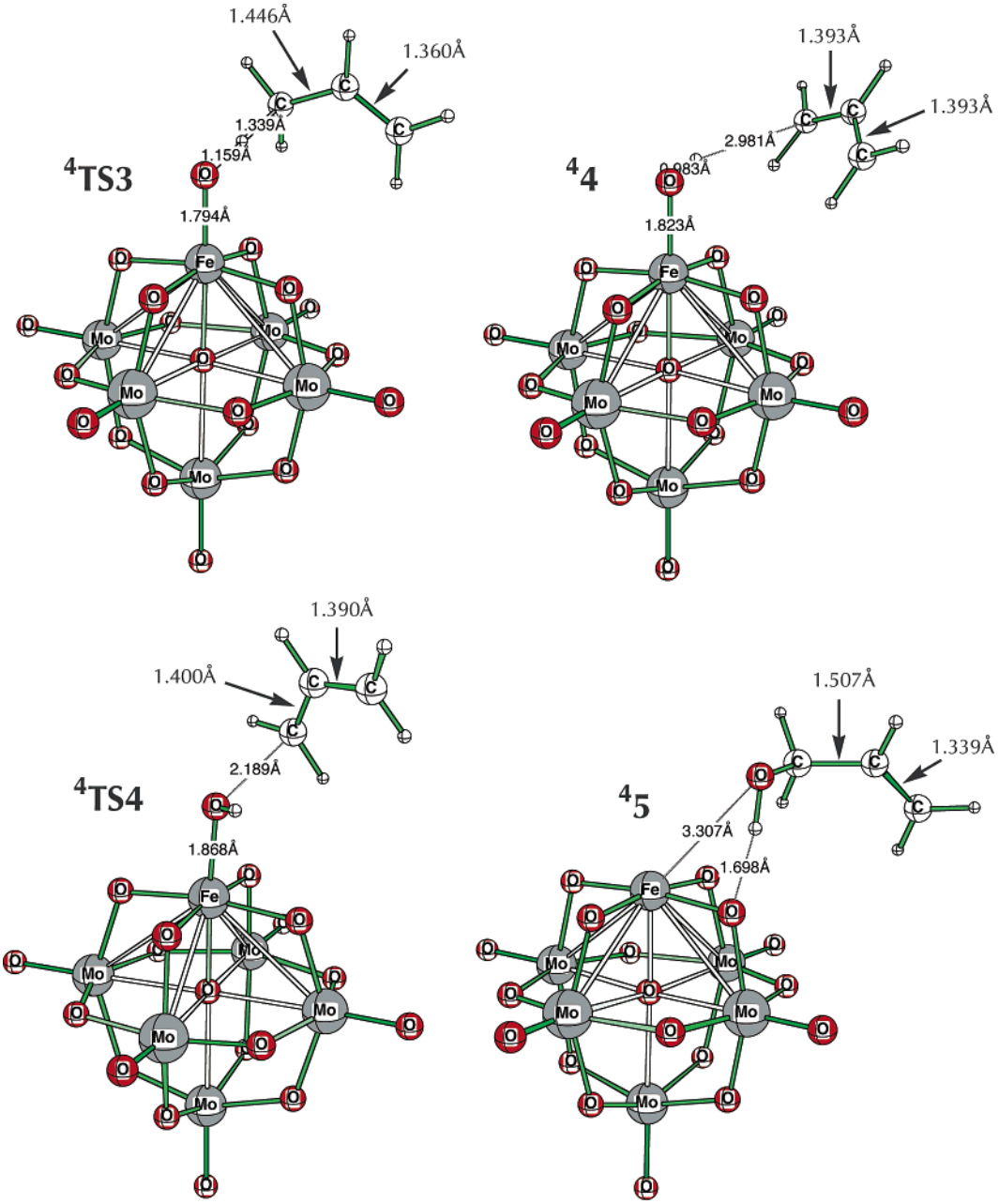

Figure 6. Structures obtained at the B3LYP/LACVP level in the quartet state for the hydroxylation process. Key distances are given in Å.

these oxidation equivalents are successively disposed of during substrate oxidation by shifting electrons from the substrate orbital to the catalyst. At the reactant state, the unpaired electrons are located in the orbitals of the $Mo_5FeO_{19}^{3-}$ reagent, two in π^* and one in δ, while the propene is closed shell and represented by the doubly occupied σ_{CH}. At this stage of the reaction, the energy difference between the quartet and the doublet spin states reflects the exchange interaction of the electrons localized on the iron−oxo moiety. Since the exchange interaction of iron is large,[23,32] the quartet−doublet energy gap will begin as a large quantity. As the reaction progresses (middle panel of Figure 8), the propene undergoes H-abstraction and an electron is shifted from the σ_{CH} orbital to one of the π^* orbitals in the quartet state and doublet (see also Supporting Information, Table 4) states. At this stage, the σ_{CH} orbital becomes a ϕ_C orbital of the allyl radical, the π^* orbital becomes a fairly localized d_π orbital on iron, and the π_{FeO} and σ^*_{CH} orbitals transform to the σ_{OH} and σ^*_{OH} orbitals of the newly formed O−H bond. Consequently, in the intermediate **4**, the POM_5-FeOH^{3-} moiety has only two unpaired electrons on the iron, and one electron now is localized on the allyl radical in the ϕ_C orbital. The exchange interaction between the electron on the radical and the electrons on iron is extremely small, and therefore, the energy gap between the doublet and the quartet state decreases drastically. In the rebound step (middle panel to right-hand panel in Figure 8), the electron of the allyl radical is shifted to the $\sigma^*_{z^2}$ orbital of the iron in the quartet state or to the π^* orbital in the doublet state; at the same time, the ϕ_C and π_{FeO} orbitals transform to the σ_{OC} and σ^*_{OC} orbitals of the newly formed C−O bond. In the product, the quartet

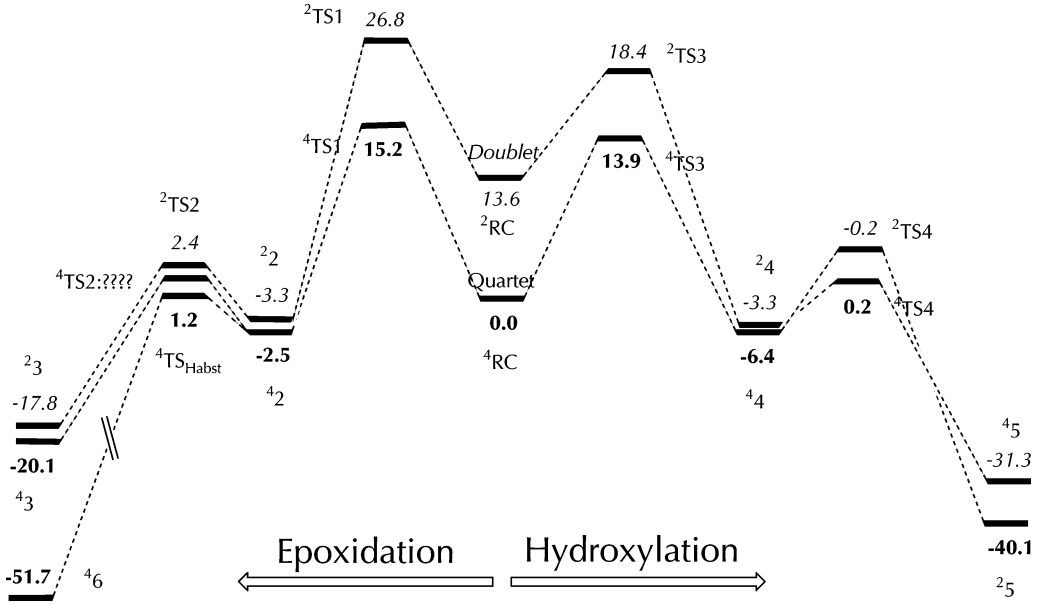

Figure 7. Reaction profile for the epoxidation and hydroxylation of propene by the Lindqvist anion $(Mo_5FeO_{19})^{3-}$. Energies are shown only at the highest level (B2+ZPC//B1). **^{4}6** is a hydroxylation product along an epoxidation path (see Figures 3 and 4 also).

Table 2. Activation Energies for the Hydroxylation and Epoxidation Processes That are Calculated at the UB3LYP/B2//B1 Level Including the ZPC and the Effect of Solvation[a]

	$\Delta E^{\ddagger}$, epoxidation		$\Delta E^{\ddagger}$, hydroxylation	
conditions	doublet	quartet	doublet	quartet
$\epsilon = 1$, vacuum	19.02/26.8	7.40/15.2	10.62/18.4	6.17/13.9
$\epsilon = 5.7$, chlorobenzene	19.83/18.7	11.82/10.7	14.46/13.3	8.51/7.4
$\epsilon = 37.5$, acetonitrile	17.17/4.4(1.3)	9.86/7.1	13.46/0.7(−2.4)[b]	7.33/4.6

[a] ZPC and solvation corrections were calculated with the B1. The barrier values (kcal/mol) are given as relative to **^{4}R**/**^{4}RC**, respectively, where **^{4}R** corresponds to the separate reagents in the quartet state, and **^{4}RC** corresponds to the quartet reactant complex. In parentheses are the barriers on the doublet surface relative to **^{2}RC**. [b] In this case, the doublet TS is lower than the clusters.

Table 3. Comparison of the Binding Energy (kcal/mol) of Propene, Ph-I, and F_5Ph-I on the Lindqvist Anion in the Two Different Spin States (doublet/quartet)

complex with	ΔE(B1)	$\Delta(E + \text{ZPC})$, B1	ΔE(B2//B1)
propene	−8.57/−8.53	−8.16/−8.01	−8.36/−8.22
Ph-I	−7.19/−8.31	−7.48/−8.29	−8.92/−10.44
F_5Ph-I	−24.73/−24.96	−24.85/−24.93	−26.82/−26.62

ferric−alcohol complex again has three electrons on the POM_5Fe moiety, while the doublet has only a single unpaired electron; the exchange interaction becomes large again and the quartet−doublet gap increases. Thus, the collapse of the spin state gap at the intermediate stage will create a TSR scenario. At this point, the doublet rebound barrier is smaller than the quartet, and therefore, we expect to see competition between the spin-state processes; passing via the doublet rebound TS would lead to more stereospecific results than via the quartet (for stereochemically labeled substrates).[30a]

The Potency of the Lindqvist Catalyst. As mentioned above, the barriers become extremely small when solvent effect is considered. The origins of this solvent effect was previously explained[6] and a brief discussion follows. When the classical Born model is used, the solvation of an ion is proportional to the square of its charge, Q^2. In the transition state for bond activation, the propene transfers some electronic charge to the Lindqvist catalyst (e.g., 0.3e for **^{4}TS3**, see Supporting Information, Table 4), and as a result, the $[POM_5FeO]^{3-}$ moiety acquires a higher negative charge ($-(3 + \Delta Q)$). Because solvation varies in proportion to the square of the charge, the transition state will be solvated more than the reactant cluster or the reactants by a quantity proportional to $-2 \times 3\Delta Q$. Thus, since the initial charge is −3, the solvation of the transition state will be amplified by a factor of 3 and in proportion to the charge increment ΔQ, which is relative to the reactant cluster. As such, we might expect a very significant solvent effect on the efficiency of the Lindqvist catalyst with preference for more polar solvents. However, these considerations do not involve entropic effects due to the changes in the solvent degrees of freedom (which are not calculated in the SCRF model). In fact, since the solvation intensifies in the transition state we expect that the solvent molecules will cluster more strongly around the POM in the transition state (electrostriction of the solvent). This will cause a large loss of degrees of freedom and will result in highly negative entropy of activation and, hence, will contribute to a significant free energy barrier. What is gained in energy because of the intensified solvation will be counterbalanced to some extent by the entropic contribution to the free energy of activation.

Why is the Lindqvist Catalyst a C−H Hydroxylation Reagent? The most practical message of this study is that the new catalyst seems to afford C−H hydroxylation even when the initial bond being activated is C=C. This unprecedented result originates in the shape of the POM_5FeO^{3-} cluster (Scheme 1). Because the cluster is small, the environment around the iron is almost purely octahedral with O=Fe−O angles of 90°. By contrast, in the large POM_{11}-FeO cluster[6] the surface is more curved and the "equatorial" −O− ligands bend away from the FeO unit. The small angles

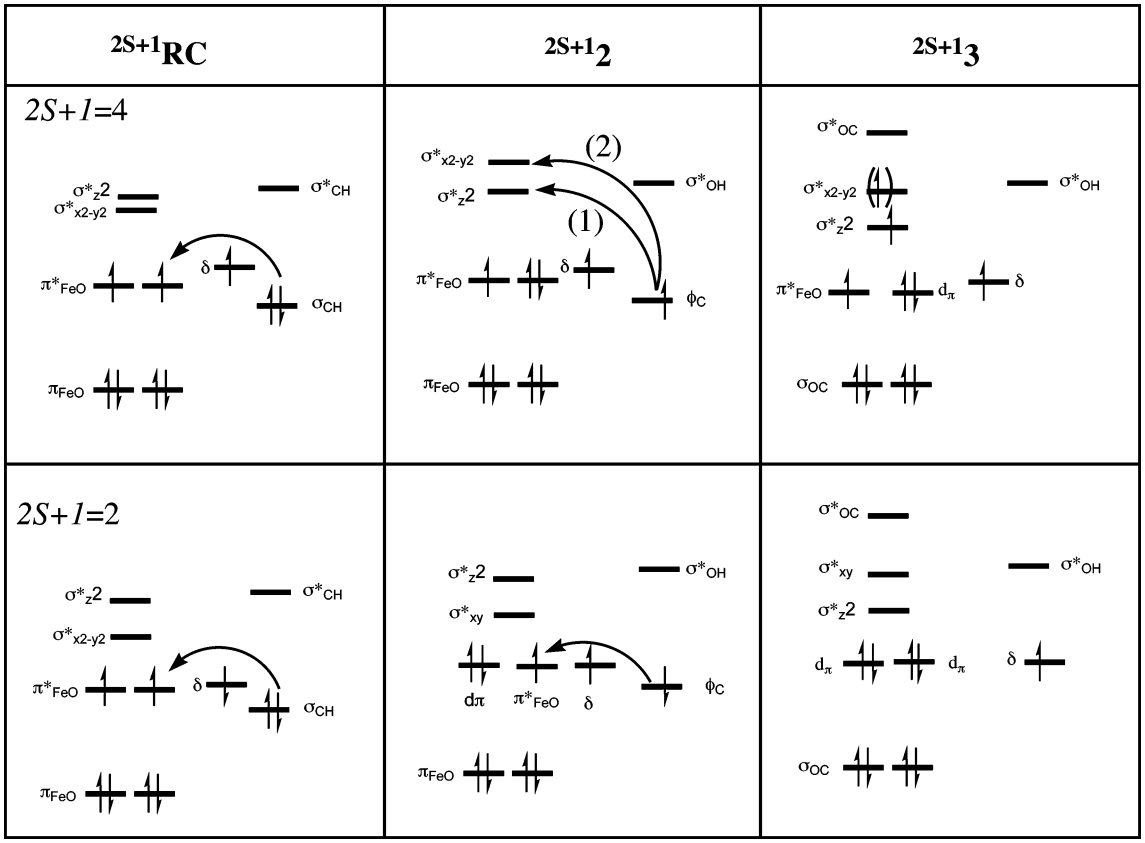

Figure 8. Orbital diagrams showing the evolution in the d-orbital occupancy along the C−H hydroxylation path (the epoxidation is analogous). In the quartet state, the arrow labeled (1) indicates the electronic reorganization leading to ^{4}**3**, whereas the arrow labeled (2) indicates the orbital occupancy during the formation of ^{4}**6**. The electron in parentheses in $\sigma^*_{x^2-y^2}$ in the quartet product refers to the occupancy in ^{4}**6**.

of the Lindqvist catalyst create proximity between the "equatorial" −O− ligands and the substrate undergoing oxidation. Because the rebound step (Figure 8) requires a shift of an electron to the $\sigma^*_{x^2-y^2}$ orbital, this electron density shift will render the equatorial oxygen ligand more negatively charged, and the structural proximity of the equatorial ligand to the propene moiety will in turn facilitate H-abstraction and conversion of the epoxidation intermediate ^{4}**2** to a hydroxylation product ^{4}**6**.

Concluding Remarks

This work involves the design of a new high-valent Fe(V)═O catalyst (POM_5−FeO^{3-}), which is based on the Lindqvist polyoxometalate, that shows promise of being stable to oxidative conditions. The calculated Mössbauer spectroscopic data may be helpful toward an eventual identification of the species. The calculations show that POM_5−FeO^{3-} is potentially a potent oxidant that is subject to strong solvent effect. Unlike the Keggin analogue that strongly prefers C═C epoxidation, the theoretically studied Lindqvist catalyst prefers C−H hydroxylation; it leads to hydroxylation products even from the pathway that starts with C═C activation.

Acknowledgment. This research was supported by the German Federal Ministry of Education and Research (BMBF) within the framework of the German−Israeli Project Cooperation (DIP). R.N. is the Rebbeca and Israel Sieff Professor of Organic Chemistry.

Supporting Information Available: Energies, coordinates, spin densities, and charges for all models and reference 19 in full. This material is available free of charge via the Internet at http://pubs.acs.org.

IC0610435